

Crystal Blocking Measurements of the Time Delay of Fission Induced by ^{32}S , ^{48}Ti , and ^{58}Ni Bombardment of W

J. U. Andersen* and J. Chevallier

Department of Physics, University of Aarhus, DK-8000 Aarhus C, Denmark

J. S. Forster

Département de Physique, Université de Montréal, Québec, Canada H3C 3J7

S. A. Karamian

FLNR, Joint Institute of Nuclear Research, 141980 Dubna, Russian Federation

C. R. Vane, J. R. Beene, A. Galindo-Uribarri, J. Gomez del Campo, H. F. Krause, E. Padilla-Rodal, and D. Radford
Oak Ridge National Laboratory, Oak Ridge, Tennessee 37831 USA

C. Broude

Physics Department, Weizmann Institute of Science, Rehovot, Israel

F. Malaguti and A. Uguzzoni

Department of Physics, University of Bologna and I.N.F.N., 40126 Bologna, Italy

(Received 30 March 2007; revised manuscript received 14 July 2007; published 15 October 2007)

The time delay in fission induced by bombardment of W with 180 MeV ^{32}S , 240–255 MeV ^{48}Ti , and 315–375 MeV ^{58}Ni has been measured by observation of crystal blocking. There is a clear narrowing and a small increase in the minimum yield of the angular dips for fission compared with scaled dips for elastically scattered ions. This is interpreted as a fission delay of about 2 as, only weakly dependent on energy and atomic number. The delay is longer by 1 to 2 orders of magnitude than obtained from standard interpretations of measurements of prescission neutrons and giant-dipole-resonance gamma rays and from calculations of the nuclear dynamics in heavy-ion reactions.

DOI: [10.1103/PhysRevLett.99.162502](https://doi.org/10.1103/PhysRevLett.99.162502)

PACS numbers: 24.75.+i, 25.70.Jj, 61.85.+p

The standard model for nuclear fission induced by ion bombardment is decay of a compound nucleus in statistical equilibrium, as introduced by Bohr and Wheeler shortly after the discovery of fission [1]. Fission competes mainly with evaporation of neutrons and after each neutron emission the nuclear temperature is significantly reduced and the lifetime for fission is strongly increased. When the fission yield has contributions from several stages in this cascade, the time scale for fission can therefore span many orders of magnitude. The existence of a tail in the time distribution, stretching to times longer than 10^{-16} s, was demonstrated by crystal blocking measurements on fission induced by light ions in the 1970s [2–4]. The observations were consistent with the average numbers of neutrons emitted before fission [5].

Crystal blocking is a time-of-flight technique. Charged particles emitted in nuclear decay at a lattice site are blocked by a row of atoms, and the blocking dip in the angular distribution is filled in if, due to the recoil in the reaction, the decaying nucleus is displaced from the row by more than about 5 pm. With increasing displacement in the range 5–100 pm the dip becomes narrower and shallower, and it vanishes for larger displacements. The shape of the dip therefore reveals whether a filling-in is due to a delay giving a recoil displacement in the range of

sensitivity or to the tail of a very broad time distribution. The latter gives an increase of the minimum yield but no narrowing, and this was seen in the early measurements [4,5].

Later studies have indicated that the Bohr-Wheeler model may break down for heavier projectiles and higher atomic numbers of the fissioning nucleus. Systematic measurements have shown that many neutrons are emitted prior to fission even for nuclei with a fission barrier so low that the fission yield should be dominated by first-chance fission. The physical explanation is thought to be a highly viscous flow of nuclear matter that delays equilibration of the fission degree of freedom in the compound nucleus. Typically, an initial time delay is introduced in the analysis, during which neutron emission but not fission is possible, and the fission width is reduced to account for diffusion backflow at the saddle. Total average fission times of a few times 10^{-20} s have been deduced from the neutron emission [6,7] and a little longer delays from emission of giant-dipole-resonance gamma rays [8]. However, there is considerable uncertainty in the interpretation. The introduction of a delay time for equilibration has been challenged [9], and fission times longer by an order of magnitude have been deduced from alternative analyses of the neutron emission [10,11].

More direct measurements of fission times for such systems have given even longer delay times. An experiment in the early 1990s on fission of highly excited uranium nuclei showed that an appreciable fraction of the fission events were slower than the atomic K -vacancy lifetime of 7 as ($1 \text{ as} = 10^{-18} \text{ s}$) [12], and this result was corroborated by later crystal blocking measurements [13]. Even more surprising were recent observations of similar long delay times for fission of superheavy nuclei with atomic number near 120, created in heavy-ion collisions [14,15]. The results have been interpreted within a compound-nucleus picture with multichance fission and a broad time distribution.

With the aim of addressing these questions, we have carried out experiments with thin tungsten crystals as targets. Earlier, we reported measurements with 170–180 MeV ^{32}S beams (performed at the tandem accelerator at the University of München, Garching), which apparently showed no lifetime effects [16]. Here we extend the measurements to ^{48}Ti and ^{58}Ni beams. A new analysis taking into account the mosaic structure of the crystal shows significant lifetime effects even for a 180-MeV S beam.

The experiments were carried out at the HRIB Facility at Oak Ridge National Laboratories. Thin (100) oriented W crystals (75 nm), grown on Mo (200 nm) on an MgO backing, were used. Ion beams of ^{32}S at 180 MeV, ^{48}Ti at 240, 245, and 255 MeV, and ^{58}Ni at 315, 330, 350, and 375 MeV bombarded the W crystal. The beam was collimated by two apertures 1.75 mm in diameter positioned 27.6 and 101.3 cm ahead of the crystal. For the ^{58}Ni experiment the collimator closest to the crystal was 1.0 mm in diameter. The crystal was tilted with the surface at 19.0° to the beam in order to observe blocking along a [111] direction at 35.3° to the crystal surface.

Elastically scattered ions and reaction products were measured in a position-sensitive gas ionization counter at 54.3° to the beam direction and 48.3 cm from the target. The detector was identical to the one used earlier [16] except that CF_4 was used as the counter gas instead of isobutane. The anode was split into ΔE (12 cm long) and E_{rest} (18 cm long) electrodes, which provided particle identification. Figure 1 shows a ΔE vs E_{rest} plot. The energy scale was calibrated from observations of 212-MeV elastically scattered Ge ions and 87-MeV W recoils. In Fig. 2 measured fission-energy spectra are compared with calculated spectra [17]. There is excellent agreement for S; for Ti and Ni the energy spectrum is modified by the polygon cut at both high and low energies, but the average energy is close to the prediction for fusion-fission reactions.

The distribution in energy of the fission fragments and the strongly correlated distribution in atomic number are needed for calculations of the blocking dips. The width scales with the Lindhard angle,

$$\psi_1 = \left(\frac{2Z_1 Z_2 e^2}{Ed} \right)^{1/2}, \quad (1)$$

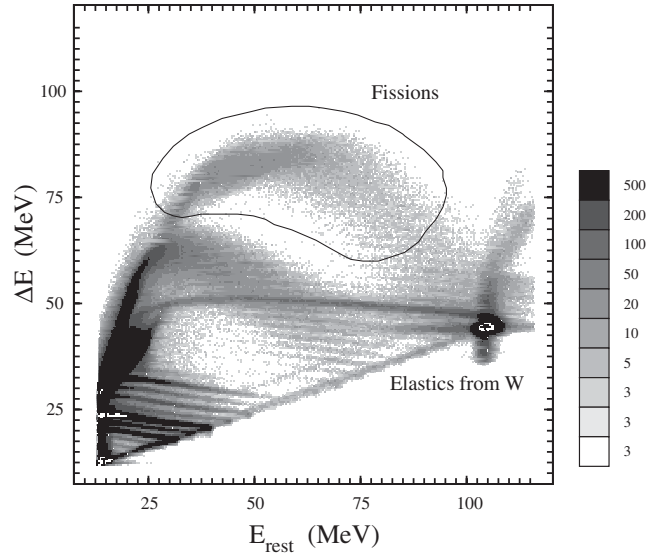


FIG. 1. The 2D spectrum for a beam of 245 MeV Ti. The intense lines to the left are from elastic recoils of Mo and W and the horizontal lines from lower- Z particles. There is a folding over of these lines at the energies where the particles are no longer stopped in the gas counter. The polygon used to select fission events is indicated.

where Z_1 and Z_2 are the atomic numbers of the particle and crystal, E is the energy, and d is the atomic spacing along the axis [18]. We have assumed a fixed average charge-to-mass ratio for the fragments and used the corresponding relation between Z and E , obtained from the fission kinematics. The corrections to the mean values of ψ_1 for the cutoff of the distributions in E and Z were less than 3%. A small deviation from the scaling with ψ_1 might be expected due to screening by projectile electrons, but our measured dips for elastic scattering of S, Ti, Ni, and Ge show no indication of such a deviation.

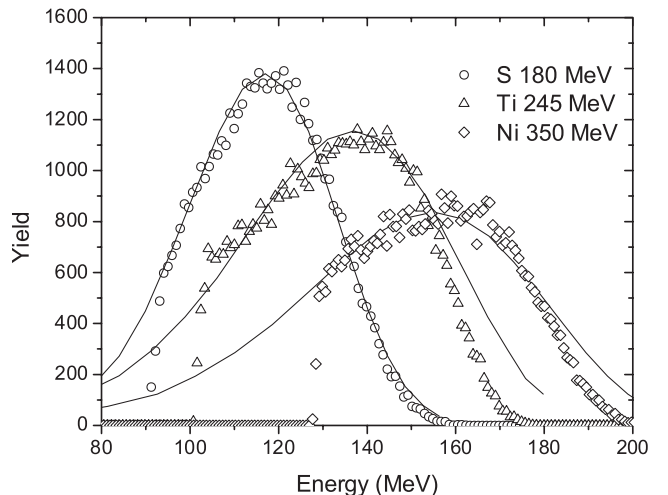


FIG. 2. Fission-energy spectra for 180 MeV S, 245 MeV Ti, and 350 MeV Ni compared with spectra calculated for a Gaussian mass distribution.

The position data were corrected on the basis of data taken with a mask placed in front of the detector [16]. These data also provided for an angular calibration of the detector. Polygon-shaped gates were set in the ΔE vs E_{rest} plot on the regions corresponding to fission and to elastic scattering from W in order to generate the 2D blocking patterns. The patterns shown in Figs. 3 and 4 were obtained from circular averages about the minimum in the 2D position spectra, and they were normalized to the yield at angles outside the blocking dip. The lifetime effects are derived from a comparison between the fission dips and blocking dips for elastic scattering, taking into account the energy dependence of the Lindhard angle ψ_1 . Fission-blocking dips for separate gates on low and high fragment energies were compared, and they are consistent with this scaling.

Figure 3(a) shows the blocking dips for elastically scattered Ni ions. The dip at the higher beam energy (350 MeV) was recorded together with fission blocking, and the lower energy (111 MeV) was chosen to give a value of ψ_1 equal to its average value for the fission fragments. The dips are compared with calculations in the continuum model with a thermally averaged multistring Lindhard

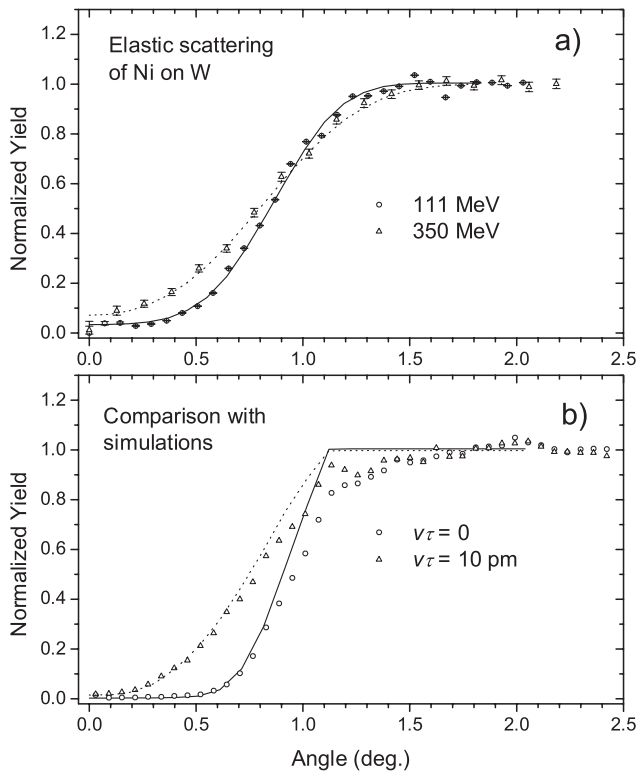


FIG. 3. (a) Blocking dips for elastic scattering of 111 MeV Ni and for 350 MeV Ni scaled in angle to the lower energy [Eq. (1)] compared with continuum-model calculations including mosaic spread and beam-spot size. (b) Comparison of continuum-model calculations (curves) with simulations for fission fragments with $Z_1 = 48$ and $E = 135$ MeV (angular resolution not included). The narrower dips correspond to an exponential displacement distribution with mean value 10 pm.

potential [5,18]. The size of the beam spot and the mosaic spread of the crystal determine the angular resolution, and both are included in the calculations. With a beam spot of 2.5 mm and a 0.35° FWHM Gaussian spread of the direction of the [111] axis the dips are reproduced very well. The mosaic spread is close to the smallest value found in a study of the conditions for epitaxial growth of W on Mo/MgO [19]. A small random component of the crystal (3%) has been included to account for crystal imperfections.

The accuracy of the continuum model can be assessed from the comparison in Fig. 3(b) with numerical simulations. The difference in the shoulder region, due to multiple scattering in the simulation [20], is reduced when the angular resolution is included in the calculations but the continuum-model dips are then slightly narrower.

Representative fission-blocking dips are shown in Fig. 4 for the three bombarding ions, compared with calculated dips with the parameters determined from fits to dips for

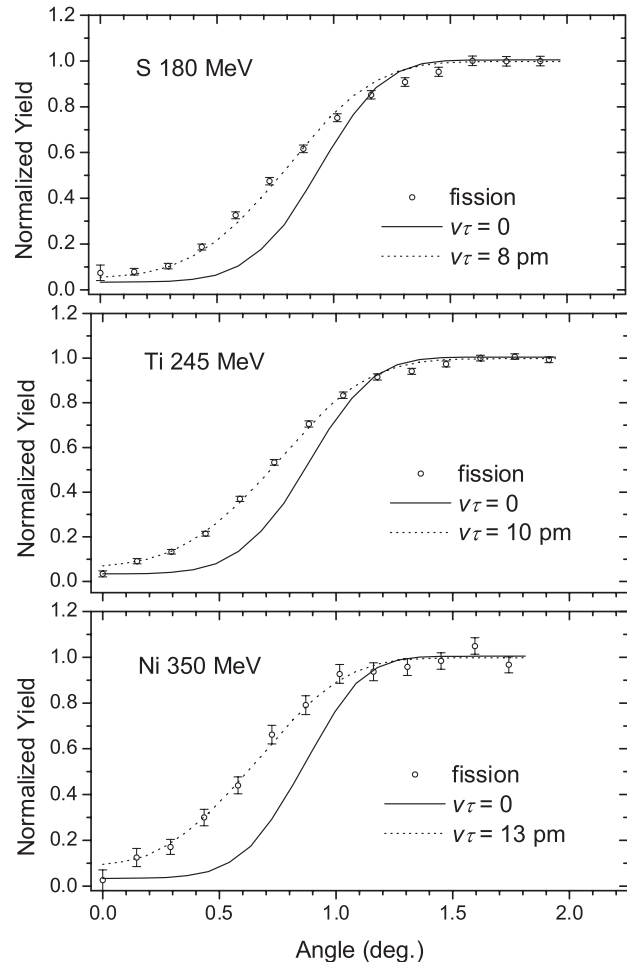


FIG. 4. Fission-blocking dips for three different bombarding ions, compared with calculations including the angular resolution and a small random component of the crystal (3%) determined from the simultaneously recorded blocking dip in elastic scattering.

elastics, as illustrated in Fig. 3(a). There is an additional average over the distribution of ψ_1 corresponding to the correlated distributions in Z_1 and E for the fragments. The measured dips are clearly narrower, and this is interpreted as an effect of a displacement of the nucleus before fission. The reason for the different conclusion in [16] for S induced fission is the comparison there of the fission dip with the elastic dip recorded at the same bombarding energy. As illustrated in Fig. 3(a), the angular resolution modifies the scaling of the dip with energy and the fission dip must instead be compared with elastic scattering at a lower energy where the value of ψ_1 is the same. According to Fig. 3, this dip is well represented by the calculation. To model the measured fission dips, we have introduced an exponential distribution of recoil distances from the atomic row. The recoil velocity components perpendicular to the axis are 4.0×10^6 m/s, 5.3×10^6 m/s, and 6.6×10^6 m/s, and the mean time delay is close to 2 as in all three cases. For Ti and Ni the dependence of the delay on the bombarding energy was found to be weak.

The measured time delays cannot be explained within the Bohr-Wheeler model with multichance fission and a broad time distribution [13–16,21]. Instead, the observations support a picture of highly damped deformation change, from the initial touching of two spheres to a more symmetric, elongated shape at scission, with simultaneous cooling by neutron emission without much influence on the dynamics [10]. There is then a nearly classical delay, with a spread from fluctuations and from the distribution in angular momentum. However, such a theoretical picture of the fission process has yet to be worked out in detail. The analysis of fission lifetimes in [10] is semi-empirical, based on data for neutron emission, and our measured delays of about 2 as are 2 orders of magnitude longer than obtained from dynamical models of heavy-ion induced reactions [22,23].

It is of great interest whether a compound system is formed in the reactions, which may survive fission and become an evaporation residue (ER). In heavy-ion reactions leading to a mononucleus with very high atomic number, the initial configuration of two touching spheres is more extended than the very compact shape at the saddle point, and this together with the high viscosity of excited nuclear matter has been suggested to be the explanation for the very low observed ER cross sections [24,25]. In [24] the additional energy barrier for formation of a compound nucleus, the “extra-extra push,” was found to be a function of a mean fissility, x_m , which takes into account the properties of both the initial configuration and the compound nucleus. The magnitude of this barrier increases dramatically in the range $x_m = 0.75$ – 0.8 , and the values of x_m for our systems are 0.72, 0.78, and 0.86 for ^{32}S , ^{48}Ti , and ^{58}Ni on ^{184}W . Hence, the reactions we have investigated are in a transition region. If there is a considerable contribution

from quasifission for the heavier projectiles, the observation of a fairly well-defined delay suggests that this delay does not depend on the formation of a compound nucleus (see also [10]). It is interesting that interpreted in such a scenario the observations by crystal blocking of delayed fission of superheavy nuclei would not imply high fission barriers from shell effects as concluded in [14,15].

We thank W.J. Swiatecki for enlightening discussions and acknowledge support from NATO Grant No. CLG980118. Research at the Oak Ridge National Laboratory was supported by the U.S. Department of Energy under Contract No. DE-AC05-00OR22725 with UT-Batelle, LLC.

*jua@phys.au.dk

- [1] N. Bohr and J. A. Wheeler, Phys. Rev. **56**, 426 (1939).
- [2] S. A. Karamian, Yu. Ts. Oganessian, and F. Normuratov, Yad. Fiz. **14**, 499 (1971).
- [3] V. V. Kamanin, S. A. Karamian, F. Normuratov, and S. P. Tretyakova, Yad. Fiz. **16**, 447 (1972).
- [4] J. U. Andersen *et al.*, Phys. Rev. Lett. **36**, 1539 (1976).
- [5] J. U. Andersen *et al.*, K. Dan. Vidensk. Selsk. Mat. Fys. Medd. **40**, 7 (1980).
- [6] D. Hilscher and H. Rossner, Ann. Phys. (Paris) **17**, 471 (1992).
- [7] D. J. Hinde, D. Hilscher, H. Rossner, B. Gebauer, M. Lehman, and M. Wilpert, Phys. Rev. C **45**, 1229 (1992).
- [8] P. Paul and M. Thoennessen, Annu. Rev. Nucl. Part. Sci. **44**, 65 (1994).
- [9] H. Hofmann and F. A. Ivanyuk, Phys. Rev. Lett. **90**, 132701 (2003).
- [10] K. Siwek-Wilczynska, J. Wilczynski, R. H. Siemssen, and H. W. Wilschut, Phys. Rev. C **51**, 2054 (1995).
- [11] V. A. Rubchenya *et al.*, Phys. Rev. C **58**, 1587 (1998).
- [12] J. D. Molitoris *et al.*, Phys. Rev. Lett. **70**, 537 (1993).
- [13] F. Goldenbaum *et al.*, Phys. Rev. Lett. **82**, 5012 (1999).
- [14] A. Drouart *et al.*, *International Symposium on Exotic Nuclei, Peterhof, 2004* (World Scientific, Singapore, 2005), p. 192.
- [15] M. Morjean *et al.*, Eur. Phys. J. D **45**, 27 (2007).
- [16] S. A. Karamian *et al.*, Eur. Phys. J. A **17**, 49 (2003).
- [17] V. E. Viola, K. Kwiatkowski, and M. Walker, Phys. Rev. C **31**, 1550 (1985).
- [18] J. Lindhard, K. Dan. Vidensk. Selsk. Mat. Fys. Medd. **34**, 14 (1965).
- [19] S. Köster, Ber. Kernforschungsanl. Jülich-Nr. 1799 (1982).
- [20] J. U. Andersen *et al.*, Nucl. Instrum. Methods Phys. Res., Sect. B **90**, 166 (1994).
- [21] J. Cabrera *et al.*, Phys. Rev. C **68**, 034613 (2003).
- [22] W. J. Swiatecki, Nucl. Phys. **A428**, 199c (1984).
- [23] V. Zagrebaev and W. Greiner, J. Phys. G **31**, 825 (2005).
- [24] J. P. Blocki, H. Feldmaier, and W. J. Swiatecki, Nucl. Phys. **A459**, 145 (1986).
- [25] W. J. Swiatecki, K. Siwek-Wilczynska, and J. Wilczynski, Phys. Rev. C **71**, 014602 (2005).